FEASIBILITY STUDY OF ZnO NANORODS FOR SENSOR APPLICATION

by

NUR SYAFINAZ BINTI RIDHUAN

Thesis submitted in fulfillment of the requirements
for the degree of
Master of Science

APRIL 2013

DECLARATION

I hereby declare that I have conducted, completed the research work and written the dissertation entitled “Feasibility Study of ZnO Nanorods for Sensor Application”. I also declared that it has not been previously submitted for the award for any degree or diploma or other similar title of this for any other examining body or University.

Name of Student: Nur Syafinaz bt. Ridhuan Signature:

Date: 30.04.2013

Witnessed by:

Supervisor: Assoc. Prof.Dr. Khairunisak Abdul Razak Signature:

Date: 30.04.2013

ACKNOWLEGMENTS

First of all, I would like to take this opportunity to thank the my supervisor, Associate Professor Dr. Khairunisak Abdul Razak and my co-supervisors Associate Professor Dr. Zainovia Lockman and Associate Professor Dr. Azlan Abdul Aziz for their supervision, invaluable guidance, unfailing help and encouragement during the master research. The information and discussion about the research work have benefited me a lot.

I appreciate technical support from technicians and other staff from School of Materials & Mineral Resources Engineering, School of Physics and Nanobiotechnology Research & Innovation (NanoBRI), INFORMM, USM who in one way or another have rendered their kind and invaluable assistance and co-operation to make my research enjoyable, informative and meaningful one. I also would like to express my gratitude to all my laboratory mates especially Ms Soo Ai, Mrs Rabizah, Ms Hajarul, Ms Hashimah and Mrs Dyana for their help in my master research.

Lastly, I special thank to my family members especially my parents for their prayer, guidance and support. I have gained some useful experience and knowledge from this research. I feel very proud to be given this opportunity. I also acknowledge financial supports from Universiti Sains Malaysia through Research University Postgraduate Research Grant Scheme (RUPRGS) and Skim Biasiswa Penyelidikan Pascasiswazah Universiti (MOSTI) scholarship throughout my study.

Thank you.

TABLE OF CONTENTS

		Page
TITLE		i
DECLARATION		ii
ACKNOWLEDGEMENTS		iii
TABLE OF CONTENTS		iv
LIST OF TABLES		vii
LIST OF FIGURES		viii
LIST OF ABBREVIATIONS		xiv
LIST OF SYMBOLS		xvi
LIST OF PUBLICATIONS		xvii
ABSTRAK		xviii
ABSTRACT		xix
CHAPTER 1: INTRODUCTION		
1.1	Research background	1
1.2	Motivation of study	4
1.3	Objectives	7
1.4	Dissertation structure	8
CHAPTER 2: LITERATURE REVIEW		
2.1	Introduction	9
2.2	Physical properties of ZnO nanostructure	11
	2.2.1 ZnO structure	12
	2.2.2 Optical and electrical properties	14
	2.2.3 Thermal properties	15
2.3	Fabrication of ZnO nanorods	16
	2.3.1 Molecular Beam Epitaxy	17
	2.3.2 Thermal evaporation / Chemical Vapor Deposition	19
	2.3.3 Pulsed Laser Deposition	22
	2.3.4 Hydrothermal	24
2.4	Theories of seeded substrate for hydrothermal growth	28

2.4.1 Fabrication methods of seeded substrate 31
2.5 Parameters of hydrothermal process 37
2.5.1 Effect of the precursor concentration 39
2.5.2 Effect of the hydrothermal bath solution pH 43
2.5.3 Effect of the hydrothermal growth duration 45
2.5.4 Effect of different doping elements on on ZnO nanorod growth 47
2.5.4.1 Effect of aluminium (Al) doped ZnO nanorods 48
2.5.4.1 Effect of indium (In) doped ZnO nanorods 50
2.6 Applications of ZnO nanorods 53
2.6.1 Introduction 53
2.6.2 Sensor requirement and characteristic 54
2.6.3 The sensor based on ZnO nanostructures 56
2.6.3.1 Ultraviolet (UV) sensor 56
2.6.3.2 Gas sensor 60
a. Reductive gas 61
b. Oxidative gas 62

CHAPTER 3: METHODOLOGY

3.1 Introduction 64
3.2 Chemical and materials 64
3.2.1 Formation of ZnO nanorods 64
3.2.2 Fabrication of interdigitated electrodes 66
3.3 Formation of ZnO nanorods 66
3.3.1 Substrate preparation 66
3.3.2 ZnO seeded substrate preparation 67
3.3.2.1 Sputtering 67
3.3.2.2 Heat treatment 67
3.3.3 Hydrothermal growth of ZnO nanorods 68
3.3.3.1 Effect of $Zn(NO_3)_2{\cdot}4H_2O$ concentration 68
3.3.3.2 Effect of hydrothermal bath solution pH 69
3.3.3.3 Effect of hydrothermal growth duration 69
3.3.3.4 Effect of different doping elements 69
3.3.4 Formation of SiO_2 layer 70

3.3.5 Fabrication of interdigitated electrodes 70
3.3.6 Flow chart 72
3.4 Characterization methods 73
3.4.1 Field Emission Scanning Electron Microscope (FESEM) equipped with Energy Dispersive X-ray Spectroscopy (EDX) 73
3.4.2 Transmission Electron Microscope (TEM) 74
3.4.3 X-Ray Diffraction (XRD) 74
3.4.4 Photoluminescence (PL) and Raman Spectroscopy 75
3.4.5 LIV Characterization System 75

CHAPTER 4: RESULTS AND DISCUSSION

4.1 Introduction 76
4.2 Formation of ZnO seed layer 77
4.3 Hydrothermal growth of ZnO nanorods 90
4.3.1 Effect of $Zn(NO_3)_2 \cdot 4H_2O$ concentration 90
4.3.2 Effect of hydrothermal bath solution pH 97
4.3.3 Effect of hydrothermal growth duration 104
4.3.4 Effect of different doping elements 112
4.3.4.1 Effect of aluminium (Al) doped ZnO nanorods 113
4.3.4.2 Effect of indium (In) doped ZnO nanorods 121
4.4 Gas sensing 129

CHAPTER 5: CONCLUSIONS AND RECOMMENDATION

5.1 Conclusions 131
5.2 Recommendation for future work 131

REFERENCES 133
APPENDICES 153

LIST OF TABLES

Table		Page
2.1	Properties of ZnO	16
2.2	Summary of other others reports on the effect of precursor concentration on the properties grow of ZnO nanorods using hydrothermal method	42
3.1	Starting chemical and material used to synthesize ZnO nanorods	65
4.1	Length and diameter of ZnO nanorods with varying zinc nitrate tetrahydrate concentrations	90
4.2	Comparison of aluminium nitrate nanohydrate concentration on grows of Al-doped ZnO nanorods.	115
4.3	Comparison of photocurrent and responsitivity of undoped and In-doped ZnO nanorods at different concentration of $In(NO_3)_2.xH_2O$	127
4.4	Comparison of current of ZnO when exposed in air and O_2 gas at 3 V	130

LIST OF FIGURES

Figure		Page
2.1	Schematic illustration of different 1D nanostructure morphologies and the terms typically used to describe them: (a) nanowires (NWs), nanofibres or whiskers; (b) nanorods (NRs); (c) nanobelts (NBs) or nanoribbons and (d) nanotubes (NTs)	10
2.2	A collection of ZnO nanostructure synthesized under controlled conditions by thermal evaporation of solid powders	12
2.3	Stick-and-ball representation of ZnO crystal structure: (a) cubic rocksalt (B1), (b) cubic zinc blende (B3), (c) hexagonal wurtzite (B4) and (d) hexagonal wurtzite structure model of ZnO	13
2.4	(a) Typical PL spectra of ZnO nanorods and (b) Energy levels of native defect in ZnO	15
2.5	(a) A typical molecular beam epitaxy system (b) schematic diagram of periodic polar inverted of ZnO templates for ordered ZnO nanorod arrays	19
2.6	Photoluminescence spectra obtained from ZnO wires of three different sizes. SEM of the typical crystalline structures at each of the spots are shown above each of the spectra	22
2.7	(a) Schematic diagram of a typical laser deposition set-up and (b) XRD patterns of the as-deposited and annealed ZnO films deposited on difference substrates showing the (002) diffraction peaks before and after annealing	24
2.8	(a) General purpose autoclave popularly used for hydrothermal treatment and hydrothermal synthesis, (b) ZnO nanorods grown via MOVPE process and (c) ZnO nanorods grown via hydrothermal process	28
2.9	SEM images of ZnO nanorods fabricated on a Si wafer with (a) bare Si wafer, (b) Al-doped ZnO film on Si wafer, (c) FESEM image of ZnO nanorods grown without seed on PET substrate	29
2.10	SEM images of ZnO buffer layer anneal duration for 2 min and 10 min. Inset SEM image of hydrothermally grown ZnO rods with anneal duration for 2 min and 10 min	32
2.11	XRD patterns of ZnO films prepared on Si substrate via spin	33

	coating and annealed under different temperatures	
2.12	SEM images of ZnO nanorods grown on Si substrate on ZnO seeds layer (a) without heat treatment and (b) with heat treatment	36
2.13	XRD pattern of corresponding ZnO nanorods of seeds layer (a) at various temperature heat treated and (b) various heat treated duration	37
2.14	Flow chart shows the possible mechanism of ZnO formation via hydrothermal reaction	38
2.15	SEM images of ZnO nanorod arrays grown under different precursor concentrations: (a) 12.5 mM, (b) 25 mM, (c) 37.5 mM and (d) 50 mM. The insets are the corresponding cross-section images of ZnO nanorod arrays	40
2.16	(a) Schematic representation of the morphology of the nanostructures, change in (b) growth rate and (c) average diameter of grow ZnO nanorods at different pH level. Inset is (b) cross sectional and (c) top-down SEM image of ZnO nanorods grow in pH 10.6	44
2.17	SEM images of ZnO nanostructures grow at hydrothermal pH of (a) 6.06, (b) 6.34, (c) 11.78 and (d) 12.89, respectively	45
2.18	The dependence of the average length and diameter of ZnO nanorods as a function of growth duration	46
2.19	Diagram of the morphology transition of ZnO nanorods with increasing reaction time	47
2.20	Schematic diagram of the proposed formation mechanism of different thickness ZnO nanoplates at different Al doping concentration (a) 0.012mmol, (b) 0.02mmol and (c) 0.04mmol	50
2.21	XRD patterns of the ZnO nanostructures (a) before and (b) after thermal annealing	51
2.22	SEM images of (a) undoped ZnO film, indium doped ZnO film with different $InCl_3$ amount (b) 0.004 M, (c) 0.0094 M, (d) 0.015 M, (e) 0.019 M and (f) electrical properties of In-doped ZnO with different In concentrations	52
2.23	Reversible switching of the ZnO nanorod network between low and high conductivity states when the 365 nm UV light was turned on and off, and the bias on the nanorods was 5 V	55
2.24	Reversibility of ZnO nanorod-on-ZnO nanofiber composite	56

	used for UV detector. ZnO nanorods were grown in 20 mM nutrient solution	
2.25	(a) Current-time curves with UV light on and off, with curve (1) refers to pure ZnO fibers magnified by 100 times and curve (2), (3) and (4) refer to ZnO nanorod-on-ZnO nanofiber using different concentration of 10 mM, 20 mM and 30 mM, respectively. Inset, formation of ZnO nanorod-on-ZnO nanofiber structure	58
2.26	(a) I-V characteristic of the nanorods measured in dark and under UV 370 nm illumination, (b) FESEM images of typical ZnOnanorods laterally aligned and (c) The dependence of photocurrent on operating time for undoped and Al-doped ZnO nanorods	60
2.27	Receptor and transducer functions of the semiconductor gas sensor	61
2.28	(a) Schematic image of reductive gas sensor (Wei *et al.*, 2011) and (b) Resistance response curves of ZnO gas sensor at different gas molecules measured at temperature 250 °C	62
2.29	(a) The schematic image of the oxidative gas sensor(Wei *et al.*, 2011) and (b) Time dependence of resistance of ZnO nanowire sensor as the gas ambient is switched to various concentrations of O_2	63
3.1	Heating profile for thermal annealing of ZnO coated Si-substrates at 400°C	68
3.2	Schematic drawing of sample placement during hydrothermal process	69
3.2	(a) Heating profile of SiO_2 formation and (b) Kinetic growth of SiO_2 layer on Si-wafer	70
3.3	Schematic illustration of interdigitated contact pattern (a) UV sensing (b) Gas sensing	71
3.4	Summary of overall process	72
4.1	Surface morphologies of ZnO seeds heat treated at different temperatures: (a) 250 °C, (b) 300 °C, (c) 350 °C, (d) 400 °C and (e) 450 °C. Heat treatment processes were carried out for 10 min in air	78
4.2	XRD spectra of ZnO seeds heat treated at different temperatures. Heat treatment processes were carried out for 10 minutes in air. Inset is the peak position (°) and intensity (a.u)	80

of (002). ■ Denote as Si substrate

4.3 FESEM images of ZnO nanorods grown on seeds heat treated at different temperatures: (a) 250 °C, (b) 300 °C, (c) 350 °C, (d) 400 °C and (e) 450 °C. The samples were hydrothermally grown for 4 hours at 80 °C 82

4.4 X-ray diffraction spectra of ZnO nanorods formed on seeds heat treated at different temperatures after hydrothermal growth at 80 °C for 4 hours. Inset is the peak position (°) and intensity (a.u) of (002). ■ Denote as Si substrate 84

4.5 (a) Room temperature PL spectra of ZnO nanorods formed on seeds heat treated at different temperatures and (b) UV peak position (nm) and intensity (a.u) with varying heat treatment temperature 86

4.6 Raman spectra of grown ZnO nanorods formed on seeds heat treated at different temperatures. The samples were hydrothermally grown for 4 h at 80 °C 88

4.7 *I–V* curves of ZnO nanorods grown on ZnO seeds heat treated at various temperatures under UV illumination (λ = 375 nm). Inset shows the responsivity (A/W) with varying heat treatment temperature at 3V 89

4.8 FESEM images of ZnO nanorods formed at different zinc nitrate tetrahydrate concentrations: (a) 0.05 M, (b) 0.1 M, (c) 0.2 M, (d) 0.3 M, and (e) 0.4 M. The samples were hydrothermally grown for 4 h at 80 °C 92

4.9 X-ray diffraction spectra of ZnO nanorods formed with varying concentration of $Zn(NO_3)_2{\cdot}4H_2O$. The samples were hydrothermally grown for 4 h at 80 °C. Inset is the peak position (°) and intensity (a.u) of (002). ■ Denote as Si substrate 93

4.10 (a) PL spectra of ZnO nanorods formed at different concentration of $Zn(NO_3)_2{\cdot}4H_2O$ at room temperature. The samples were hydrothermally grown for 4 h at 80 °C and (b) UV peak position (nm) and intensity (a.u) with varying $Zn(NO_3)_2{\cdot}4H_2O$ concentration 95

4.11 *I–V* curves of ZnO nanorods grown at different $Zn(NO_3)_2{\cdot}4H_2O$ concentrations under UV illumination (λ = 375 nm). Inset show the responsivity (A/W) with varying $Zn(NO_3)_2{\cdot}4H_2O$ concentration at 3V 97

4.12 FESEM images of ZnO formed in hydrothermal solution containing 0.1M $Zn(NO_3)_2{\cdot}4H_2O$ and 0.1 M HMT at different 99

pH: (a) pH 3, (b) pH 5, (c) pH 7, (d) pH 9, (e) pH 11 and f) pH 13. The samples were hydrothermally grown for 4 h at 80 °C

4.13 X-ray diffraction spectra of ZnO synthesized in hydrothermal precursor solution containing 0.1 M $Zn(NO_3)_2{\cdot}4H_2O$ and 0.1 M HMT at different pH. Inset is the peak position (°) and intensity (a.u) of (002).■ Denote as Si substrate 101

4.14 Room-temperature PL spectra of ZnO nanorods formed at different hydrothermal bath solution pH. The samples were hydrothermally grown for 4 h at 80 °C. Inset is the UV peak position (nm) and intensity (a.u) with varying hydrothermal bath solution pH 102

4.15 *I–V* curves for ZnO nanorod sensors under UV illumination (λ = 375 nm) at different hydrothermal solution pH values. Inset show the responsivity (A/W) with varying hydrothermal bath solution pH at 3V 104

4.16 FESEM images of ZnO nanorods formed at 80 °C with varying hydrothermal growth duration: (a) 1 h, (b) 4 h, (c) 8 h, (d) 16 h, and (e) 24 h 106

4.17 X-ray diffraction spectra of ZnO synthesized with varying hydrothermal growth duration. The samples were hydrothermally grown at 80 °C. Inset is peak position (°) and intensity (a.u) of (002).■ Denote as Si substrate 107

4.18 Room-temperature photoluminescence spectra of ZnO nanorods formed at different hydrothermal growth duration. The samples were hydrothermally grown at 80 °C. Inset UV peak position (nm) and intensity (a.u) with varying hydrothermal growth duration 108

4.19 *I–V* curves for ZnO nanorod sensors under UV illumination (λ = 375 nm) at different hydrothermal growth durations. Inset show the responsivity (A/W) with varying hydrothermal bath solution pH at 3V 109

4.20 *I–V* curves for the ZnO film and ZnO nanorod sensors under UV illumination (λ = 375 nm) 111

4.21 TEM images of ZnO nanorods grow via hydrothermal at growth temperature of 80 °C 112

4.22 FESEM images of (a) undoped and Al-doped ZnO nanorods growth with different concentrations of aluminium doping: (b) 1 mM, (c) 5 mM, (d) 10 mM, (e) 15 mM and (f) 20 mM. The samples were hydrothermally grown for 4 h at 80 °C 115

4.23	XRD spectra of (a) undoped ZnO nanorods and Al-doped ZnO nanorods growth with different concentrations of $Al(NO_3)_3.9H_2O$. The samples were hydrothermally grown for 4 h at 80 °C. Inset is peak position (°) and intensity (a.u) of (002). ■ Denote as Si substrate	117
4.24	Room temperature PL emission spectra for undoped and Al-doped ZnO nanorods growth with different concentration of aluminium doping. Inset UV peak position (nm) and intensity (a.u) with varying concentration of aluminium doping	118
4.25	Current-voltage (*I-V*) characteristics of undoped and different concentrations of Al-doped ZnO nanorods measured in dark and under UV light ($\lambda = 375$ nm). Inset shows the responsivity (A/W) as a function of as a function of different concentration of aluminium doping at 3V	120
4.26	A TEM image of Al-doped ZnO nanorods grown using hydrothermal with 5 mM $Al(NO_3)_3.9H_2O$. The sample was hydrothermally grown for 4 h at 80 °C	120
4.27	FESEM images of In-doped ZnO nanorods growth with different concentrations of indium doping: (a) 1 mM, (b) 5 mM, (c) 10 mM, (d) 15 mM and (e) 20 mM. The samples were hydrothermally grown for 4 h at 80 °C	122
4.28	XRD spectra of (a) undoped ZnO nanorods and In-doped ZnO nanorods growth with different concentrations of $In(NO_3)_2.xH_2O$. The samples were hydrothermally grown for 4 h at 80 °C. Inset is peak position (°) and intensity (a.u) of (002). ■ Denote as Si substrate	124
4.29	Room temperature PL emission spectra for undoped and In-doped ZnO nanorods growth with different aluminium concentration. Inset shows UV peak position (nm) and intensity (a.u) as a function of different concentration of indium doping.	126
4.30	Current-voltage (*I-V*) characteristics of undoped and different concentrations In-doped ZnO nanorods at measured in dark and under UV light ($\lambda = 375$ nm). Inset shows the responsivity (A/W) as a function of as a function of different concentration of indium doping at 3V	128
4.31	TEM image of 5 mM In-doped ZnO nanorod. The sample was hydrothermally grown for 4 h at 80 °C	128
4.32	*I-V* characteristic of the fabricated ZnO nanostructure oxygen (O_2) sensor	130

LIST OF ABBREVIATIONS

1D	One Dimensional
A	Current
Al	Aluminium
$Al(NO)_3.9H_2O$	Aluminium nitrate nanohydrate
Ar	Argon
$C_2H_{12}N_4$	Hexamethylamine
CVD	Chemical Vapor Deposition
FESEM	Field Emission Scanning Electron Microscope
Ga	Gallium
H^+	Hydrogen ions
H_2O_2	Hydrogen peroxide
HCl	Hydrochloric Acid
HMT	Hexamethylenetetramine
In	Indium
$In(NO_3)_2.xH_2O$	Indium nitrate hydrate
I-V	Current-Voltage
M	Molar
MBE	Molecular Beam Epitaxy
Min	Minutes
mM	miliMolar
MOCVD	Metal Organic Chemical Vapor Deposition
NaOH	Sodium Hydroxide
nm	nanometer
O_2	Oxygen gas
OH^-	Hydroxyl ions
PL	Photoluminescence
PLD	Pulsed-Laser Deposition
PTFE	Polyetetraflouroethylene
R	Responsivity

RCA	Radio Corporation of America
RF	Radio Frequency
SEM	Scanning Electron Microscope
Si	Silicon
TEM	Transmission Electron Microscope
UV	Ultraviolet
XRD	X-Ray Diffraction
$Zn(NO_3)_2.4H_2O$	Zinc nitrate hydrate
Zn^{2+}	Zinc ions
μm	micrometer

LIST OF SYMBOLS

°C	Degree Celsius
°C/min	Degree Celsius per Minute
Å	Armstrong
λ	Lambda
2θ	Two theta
A/W	Current per Power

LIST OF PUBLICATIONS

Nur Syafinaz Ridhuan, Khairunisak Abdul Razak, Zainovia Lockman, Azlan Abdul Aziz, Structural and morphology of ZnO nanorods synthesized using ZnO seeded growth hydrothermal method and its properties as UV sensing, Plos One, November 2012, Volume 7, Issue 11, e50405

Nur, S. R., Zainovia, L., Aziz, A. A. &Razak, K. A. (2012). Properties of ZnO nanorods arrays growth via low temperature hydrothermal reaction. Advanced Materials Research

Ridhuan, N. S., Fong, Y. P., Lockman, Z. &Razak, K. A. (2011). Formation of ZnO nanorods via seeded growth hydrothermal reaction. Applied Mechanics and Materials

Ridhuan Nur Syafinaz, Abdul Razak Khairunisak, Abdul Aziz Azlan, Lockman Zainovia, Properties of In-doped ZnO nanorods synthesized using seeded growth hydrothermal method, The 6th International Conference on Technological Advances of Thin Films and Surface Coatings, 14-17 July 2012, Singapore, p. 218-219

Nur Syafinaz Ridhuan, Zainovia Lockman, Azlan Abdul Aziz, Khairunisak Abdul Razak, Formation of Al-doped ZnO nanorods via low temperature hydrothermal method, International Conference on X-Rays & Related Techniques in Research& Industry 2012 (ICXRI 2012), 3 –5th July 2012, Vistana Hotel, Penang, p.135

KAJIAN KEBOLEHUPAYAAN NANOROD ZnO UNTUK APLIKASI PENGESAN

ABSTRAK

Zink oksida (ZnO) menerima faedah yang besar kerana sifat elektronik, optik dan fotonik mereka yang cemerlang, serta jurang jalur lebar sebanyak 3.2 eV yang memberi manfaat bagi aplikasi gelombang pendek optoelektronik. Kerja ini menggambarkan sifat 1D ZnO tatasusunan nanorod (NR) yang disintesis menggunakan tindak balas suhu rendah hidroterma yang mudah pada benih ZnO/Si wafer. ZnO benih yang dirawat haba digunakan untuk mengawal morfologi dan sifat-sifat ZnO nanorod. Beberapa parameter hidroterma dikaji terhadap pertumbuhan ZnO NR dan prestasinya terhadap pengesan ultraungu (UV) dan O_2 gas. Suhu optimum rawatan haba untuk menghasilkan benih ZnO yang bersaiz nano adalah 400 °C. Bagi menghasilkan nanorod yang berhujung tumpul (~770 nm panjang dan ~80 nm diameter) tindak balas hidroterma optimum ialah 0.1 M zink nitrat, pH 7, dan tempoh pertumbuhan 4 jam dengan responsiviti yang tinggi pada 3.61×10^{-5} A/W bagi pengesanan UV. Pengesan UV berpretasi tinggi pada ZnO NR berbanding ZnO filem adalah disebabkan kawasan permukaan berbanding jumlah yang besar. Kepekatan optimum dopan Al ialah 5 mM dan In ialah 5 mM didapati dapat meningkatkan sifat pengesan UV daripada ZnO NR. Tambahan pula, sensitiviti tinggi pada ZnO nanorod (1.41×10^{-7}A) berbanding ZnO filem (1.85×10^{-6} A) dalam persekitaran O_2 disebabkan luas permukaan yang tinggi disediakan bagi tindak balas gas O_2. Arus tinggi pada Al dopan ZnO NRs (6.88×10^{-7} A) dan In dopan ZnO NRs (2.90×10^{-7} A) berbanding ZnO NR adalah disebabkan lebihan electron.

FEASIBILITY STUDY OF ZnO NANORODS FOR SENSOR APPLICATION

ABSTRACT

Zinc oxide (ZnO) has received a considerable interest because of its excellent electronic, optical, and photonic properties, as well as a wide band gap of 3.2 eV that benefits short-wavelength optoelectronic applications. This work describes the properties of 1D ZnO nanorods (NRs) arrays synthesized using a low temperature hydrothermal method on ZnO seeds/Si wafer. Heat treated ZnO seeds layer were used to control the morphology and properties of the grown ZnO nanorods. The effects of several hydrothermal parameters on the formation of ZnO NRs and its performance for ultraviolet (UV) and O_2 gas sensing were studied. The optimum heat treatment temperature to produce uniform nanosize ZnO seeds was 400 °C. The optimum hydrothermal reaction temperature to produce blunt tip-like nanorods (~770 nm long and ~80 nm diameter) were 0.1 M zinc nitrate, pH 7, and 4 h of growth duration with a high responsivity at 3.61×10^{-5}A/W of UV sensing. High performance UV sensing of ZnO NRs compared to ZnO film is due to the large surface area to volume. The optimum doping concentration of Al and In is 5 mM with higher responsitivity of 23.56 A/W and 1.48 A/W, respectively, compared to undoped ZnO NRs. Furthermore, high sensitivity of ZnO nanorods (1.41×10^{-7}A) compared to ZnO film (1.85×10^{-6} A) in O_2 environment was observed that was attributed to high surface area available for O_2 gas reaction. High current of Al-doped ZnO NRs (6.88×10^{-7} A) and In-doped ZnO NRs (2.90×10^{-7} A) compared to ZnO NRs was observed due to excess electron presence.

CHAPTER 1

INTRODUCTION

1.1 Research background

Semiconductor materials have been widely used in various applications including electronic, photonic, energy, and catalytic. Since the last decades, nanotechnology and nanomaterials have become a major interest of scientific and technical activities. This is due to unique properties of nanostructure and outstanding performance of nano-scale devices compared to their bulk counterparts. Nanostructure can be defined as a structure that has at least one dimension between 1 and 100 nm (Xia *et al.*, 2003). Unique properties in nanostructure materials are due to large surface-to-volume ratio, quantum confinement and change of the force/energy with the shrinking scale. ZnO nanostructure becomes the most potential candidates owing to its important physical properties and application aspect compared to others semiconductor materials. In addition, ZnO nanostructure also has advantages of low toxicity, good thermal stability, good oxidation resistibility and good biocompatibility material, which is a good candidate to construct functional devices (Mamat *et al.*, 2012, Wei *et al.*, 2011). ZnO is a transparent wide band gap semiconductor of 3.3 eV at room temperature with a large exciton binding energy of 60 meV which is larger than the thermal energy at room temperature (26 meV) and a high optical gain ($300cm^{-1}$) (Mamat *et al.*, 2012, Polsongkram *et al.*, 2008). Due to its outstanding properties, ZnO-based materials have been developed and utilised in many applications such as field-effect transistor (Hoffmann *et al.*, 2011), dye-sensitized solar cells (DSSCs) (Al-Hajry *et al.*, 2009), light emitting diodes (Kim *et*

al., 2002), sensing application including chemical, biological and ultraviolet sensors (Fang *et al.*, 2009, Mamat *et al.*, 2011b, Qi *et al.*, 2008, Wahab *et al.*, 2009).

Much attention has been placed on ZnO nanostructures for sensing applications. ZnO nanostructure can be used as ultraviolet sensor owing to its wide band gap of 3.3 eV. The use of ZnO for UV sensor application does not require ultra-high vacuum environment and high voltage supply as in the Si-based UV sensor. Moreover, ZnO is chemically and thermally stable, which advantages for devices operate in a harsh environment (Liu *et al.*, 2010a). UV sensing has been widely used in various commercial and military applications including fire alarms, pollution monitoring, water sterilization, space technology and early missile plume detection (Liu *et al.*, 2010a, Mamat *et al.*, 2011b). Apart from application in UV sensing, ZnO also becomes a promising candidate for gas sensing application due to its high sensitivity towards many target gases in conjunction with easy fabrication methods and low cost of fabrication (Arafat *et al.*, 2012). Detection of target gas molecules is usually achieved by measuring the change in resistivity of ZnO with the reversible chemisorptions of target gas at the surface of ZnO that produces large and variation of conductance of ZnO (Heo *et al.*, 2006, Ozgur *et al.*, 2010). Heo *et al.* (2006) suggested several possible gas sensing mechanisms including changes in surface or grain boundary conduction by gas adsorption/desorption, exchange of charges between adsorbed gas species and ZnO surface caused change in depletion depth, and desorption and adsorbed surface oxygen and grain boundary of ZnO. Detection of target gas can be divided into two categories; i) oxidizing gas or electron acceptors such as O_2, O_3, NO_2 and NO and ii) reducing gas or electron donors such as H_2, CO, CO_2, H_2S, NH_3 and CH_4 (Arafat *et al.*, 2012, Wei *et al.*, 2011). These gases were

emitted from various sources which could be hazardous to human being and environment while others can be used as measures to diagnose the state of their sources. Most of these gases presence at low concentration, therefore a good sensing characteristic is required for monitoring.

1D nanostructures ZnO such as nanorods, nanowires, nanotubes and nanobelts have become the focus in research due to their large surface-to-volume ratio and direct carrier conduction in 1D nanostructure (Dhara and Giri, 2012). In this work, nanorods structures have been studied. Generally, electrical and optoelectronic properties of nanodevices are dependent on the surface of nanostructure material. As the surface-to-volume ratio of nanorods is high, the surface states of ZnO influence optical absorption, luminescence, photodetection as well as other properties (Dhara and Giri, 2012). Owing to its unique properties, ZnO nanorods have been synthesized using several techniques that can be divided into two categories. First, vapour phase growth that is a combination reaction between metal vapour source and oxygen gas or other gas. Several techniques involve are thermal evaporation (Srivatsa *et al.*, 2011, Umar *et al.*, 2009), chemical vapour deposition (Galoppini *et al.*, 2006, Shalish *et al.*, 2004), pulse laser deposition (Liu *et al.*, 2006, Okada *et al.*, 2005) and molecular beam epitaxy (Iwata *et al.*, 2005, Lee *et al.*, 2008). Second, solution phase growth, which is growth method that requires low temperature growth. This method reduces the complexity and cost. Several techniques in the solution phase growth are sonochemical method (Mamat *et al.*, 2011a), surfactant-assisted growth (Sun *et al.*, 2003) and hydrothermal (Lockman *et al.*, 2010, Tan *et al.*, 2010, Wahab *et al.*, 2009).

1.2 Motivation of study

In this work, hydrothermal method is chosen to grow ZnO nanorods using seeded substrate. Hydrothermal method is a simple and efficient method to grow ZnO single crystal. Moreover, hydrothermal routes are more convenient and economical for large-scale production of well aligned ZnO nanorods. However, in order to control the uniformity of distribution, orientation and aspect ratio of ZnO nanorods grow on substrate via hydrothermal reaction, a seeded substrate is required. Seeded substrates could be prepared by pre-coating the substrate with seeds of the same material as nanocrystals, since this is an effective way to control the formation of nanorods. In the chemical growth method of oxide material, homogeneous nucleation of solid phase in solution is usually hindered due to the high surface energy in forming small nuclei (Guo *et al.*, 2005). As a result, heterogeneous nucleation is preferable due to low interfacial tension which is caused by smaller surface energy at water/oxide interface (Vayssieres, 2007). Thus, most of the hydrothermal growth of ZnO nanorods onto substrates requires pre-coating the substrate with ZnO buffer layer prior to the hydrothermal synthesis in order to promote a high oriented growth (Loh and Chua, 2007). The use of silicon (Si) wafer as a substrate to grow ZnO nanorods is preferable since it is low cost and well established technology of substrate (Shen *et al.*, 2006, Zhao *et al.*, 2009). However, deposition of ZnO film onto Si-substrate as a seed layer without any heat treatment process causes several problems due to its large difference of lattice mismatch and thermal expansion coefficients between Si and ZnO films. Li *et al.* (2010) and Song *et al.* (2008) used ZnO buffer layer deposited onto Si-substrate without any heat treatment process prior to growing ZnO nanorods via hydrothermal method whereby columnar ZnO nanorods were formed. Formation of columnar nanorods could affect

the electron transportation throughout the nanorods, hence influenced the conductivity properties of ZnO. Li *et al.* (2010) and Song *et al.* (2008) works studied the effect of heat treatment on ZnO seeds layer on the growth of ZnO nanorods via hydrothermal method. The ZnO nanorods formed were well aligned. These results show the importance of the heat treatment of ZnO buffer layer prior to be used in hydrothermal process.

Apart from the influence of seeded substrate, the growth of ZnO in hydrothermal reaction is also dependent on the external parameters. In order to gain control over the morphology of ZnO nanorods formed via hydrothermal reaction, the precursor and chelating agent used (Habibi *et al.*, 2009, Shouli *et al.*, 2010), growth time (Cross *et al.*, 2005, Vernardou *et al.*, 2007), concentration of precursor (Jeong *et al.*, 2011, Vayssieres, 2003), hydrothermal growth temperature (Kar *et al.*, 2009, Zhang *et al.*, 2007) and pH of the solution (Song *et al.*, 2008, Wu *et al.*, 2010). Lockman *et al.* (2010) have been grown ZnO nanorods on a seeded Zn sheet with the optimum ZnO seeds formation was obtained after oxidation at 300°C of Zn sheet. Further increased the oxidation temperature beyond 300 °C formed ZnO flakes rather than spherical ZnO seeds. Tan *et al.* (2010) have used a PTFE substrate with coated ZnO seeds layer oxidized at 300°C. In both works, the potential applications for sensors using ZnO nanorods have not been investigated because of substrate unsuitability. Liu *et al.* (2009) produced an array of ZnO nanorods on ZnO seeded Si-substrate. ZnO seeds layer was prepared by annealing the sputtered ZnO film at different annealing temperature. The length of ZnO nanorods increased with increasing annealing temperature, reaching 501 nm for seeds annealed at 600 °C. However, the use of high annealing temperature can degrade the ZnO buffer layer

which could influence and limit the application of ZnO nanorods. This degradation could be induced by interdiffusion between the buffer layer and Si substrate, and also by the thinning the buffer layer through evaporation at high temperature (Zhao *et al.*, 2009). Although Liu *et al.*, (2009) obtained almost similar results on the effect of the heat treatment of a seeded substrate; the effect of hydrothermal parameters has not been studied. The electrical properties of the produced ZnO have also not been reported. ZnO is naturally an n-type semiconductor. However, undoped ZnO usually shows a low conductivity, low optical properties and low resistance against corrosive environment. In order to enhance desired properties, several factors need to be considered including an appropriate growth technique, control of synthesis condition and selective incorporation of foreign atom (doping) (Yogamalar and Chandra Bose, 2011). Doping ZnO with different elements is an accepted approach to modify and improve the electrical properties (n-type or p-type), optical properties and magnetic properties of ZnO (Mamat *et al.*, 2010, Mashkoor *et al.*, 2009, Yogamalar and Chandra Bose, 2011). Intentional doping with group III elements such as gallium (Ga), aluminium (Al) and indium (In) is believed to be able to increase the conductivity of ZnO due to the presence of extra valence electron. Although several reports demonstrate doping of group III elements but to our knowledge limited works have been performed on using heat treated ZnO seeded substrate to grow ZnO doped nanorods via hydrothermal method.

Sensing properties are dependent on final morphology and crystallinity of ZnO nanorods formed. This is because by modifying the surface of nanorods, it will influence the relationship between surface defects and surface adsorption of gas molecules from the atmosphere. In addition, the homogeneity and density of ZnO

nanorods formed could produce large sensing signals due to large surface coverage and nanorods density (Mamat *et al.*, 2012). The present study reports the fabrication and characterization of ZnO nanorods using a hydrothermal method on seeded ZnO substrates. The effects of hydrothermal parameters (including heat-treatment temperature, zinc nitrate ($Zn(NO_3)_2$) concentration, pH of hydrothermal bath solution, and hydrothermal reaction time) on ZnO nanorod formation were systematically studied. The UV-sensing properties of all samples were correlated with their structure and morphology. The final morphology and crystal structure of ZnO nanorods were found to affect the sensing properties. Although several works have reported improvements in UV-sensing properties when using ZnO nanorods (Ji *et al.*, 2009, Li *et al.*, 2009, Liu *et al.*, 2010b, Mamat *et al.*, 2011b), to the authors' knowledge, reports on using ZnO nanorods produced at different hydrothermal parameters are very limited.

Hence, the purpose of this research is to optimize the fabrication condition of ZnO nanorods by hydrothermal reaction using a heat treated seeds in a simple and efficient way to be used in various sensing applications (ultraviolet and gas). This research has developed a low cost, fast response and high sensitivity sensors at room temperature.

1.3 Objectives

The main objectives of this research are:

i. To study the effect of synthesis parameters on ZnO nanorods properties using hydrothermal method on ZnO seeded substrate on silicon wafer

ii. To study the effect of Al and In doping concentrations on ZnO doped properties and morphology

iii. To investigate the characteristic and properties of ZnO nanorods and Al and In-doped ZnO for sensor applications

1.4 Dissertation structure

This dissertation consists of five chapters. Chapter 1 discusses on the introduction, objectives and research motivation of the research. Literature review of related works is discussed in Chapter 2. In Chapter 3, experimental details and characterization approaches are explained in details. In Chapter 4, the results and discussion of this research are presented. Finally, conclusion and recommendations of future work are stated in Chapter 5.

CHAPTER 2

LITERATURE REVIEWS

2.1 Introduction

Semiconductor materials have been widely used in electronic, photonic, catalytic and energy related applications (Barth *et al.*, 2010). Miniaturization of devices has lead to extensive study of semiconductor in nanosize range. Reducing size of semiconductor materials up to nanometer scale directly affect the appearance of quantum effect which is attributed to the limited motion of electrons in the confined dimensions of nanomaterials (Barth *et al.*, 2010). As a result, excellent characteristics have been obtained compared to those of the corresponding material in bulk size, which ultimately improve the device performance. Moreover, desired properties for a specific application could be achieved by controlling the dimension as well as composition of semiconductor structures. Formation of nanostructure can be divided into several classes: two-dimensional (2D) structure, one-dimensional (1D) structure and Zero-dimensional (0D) structure. The 2D structure involves morphology of thin film with several nanometers thickness and usually deposited on bulk material. The properties 2D structure are dependent on surface and interface effect while confinement of electron occurs in the direction perpendicular to the film and could behave like bulk material. The 1D structure has morphology of cylinder such as wires, rods and tubes with diameter in nanometer range and length typically in micrometer range. Confinement effect of electrons could appear in transverse direction while electrons are free to move in one dimension/along the structure. The 0D structure has morphology of nanoparticles, cluster, colloids and nanocrystals

which are composed of several 10-1000 atoms. Confinement of electrons happens in all directions. Figure 2.1 shows several nanostructures classified as 1D structure (Barth *et al.*, 2010).

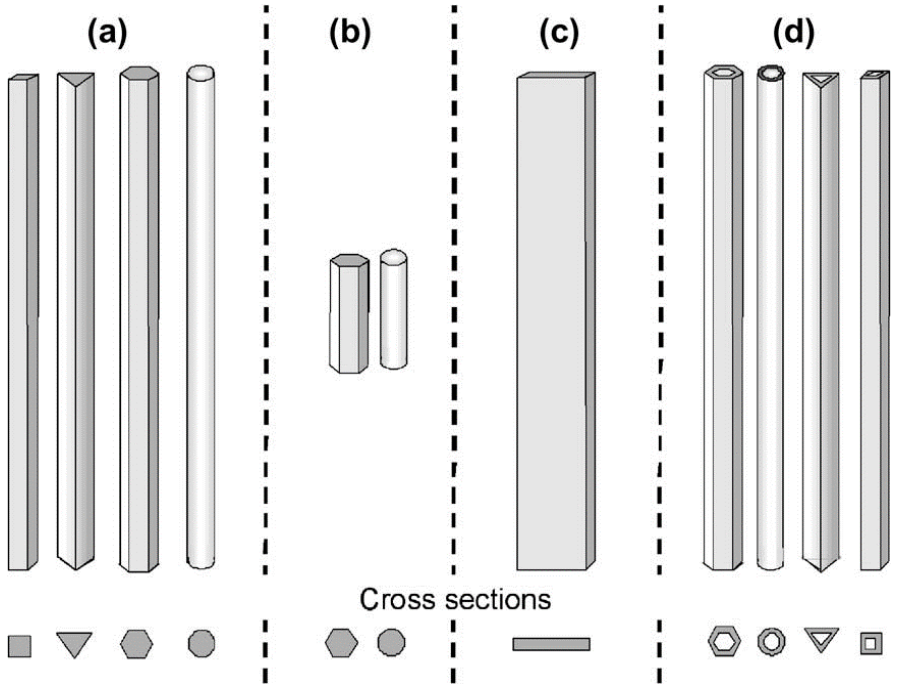

Figure 2.1: Schematic illustration of different 1D nanostructure morphologies and the terms typically used to describe them: (a) nanowires (NWs), nanofibres or whiskers; (b) nanorods (NRs); (c) nanobelts (NBs) or nanoribbons and (d) nanotubes (NTs) (Barth *et al.*, 2010)

1D nanostructure has gained much attention among researchers due to its distinctive application in mesoscropic physics and fabrication of nanoscale devices compared to other types of nanostructure (Xia *et al.*, 2003). In comparison with 0D and 2D nanostructure, 1D provides a good system to explore such as dependence of electrical and thermal transport, mechanical properties on dimensionality and size reduction. However, the formation of 1D nanostructure with well-controlled dimension, morphology, phase purity and chemical composition requires great

efforts. Chemical synthesis process could provide an alternative method to synthesis 1D nanostructure with large quantities from various ranges of materials with repeatability and at reasonably low cost for a high-volume production (Xia *et al.*, 2003).

Among available semiconductor nanostructures, zinc oxide (ZnO) is of interest owing to its unique properties and versatile applications. In this chapter, literature review on background studies, properties and formation of ZnO nanorods are explained. This is followed by a comparison of the various methods used to synthesis ZnO nanorods with the main focus on a hydrothermal method. Finally, the applications of ZnO nanorods as ultraviolet and gas sensor are addressed.

2.2 Physical properties of ZnO nanostructure

ZnO has gained much attention due to its excellent optical, electronic, sensing and catalytic properties. With large exciton binding energy of 60 meV, ZnO could lead to lasing action causes by exciton recombination interaction (Mamat *et al.*, 2012, Wang *et al.*, 2007b). In semiconductors, exciton recombination is more efficient radiative process and also it can lower threshold lasing. In addition, efficient excitonic laser process could be achieved at room temperature by having a binding energy of exciton larger than the thermal energy at room temperature (26 meV) (Loh and Chua, 2007). Therefore, ZnO result in efficient of near band-gap recombination at room temperature due to its large binding energy. Naturally, ZnO behaves as an n-type semiconductor material that is transparent to visible light which has a good ultraviolet absorption. Moreover, ZnO is biocompatible and biosafe which can be used in biomedical and coating applications (Mamat *et al.*, 2012). ZnO is a versatile

material that has various growth morphologies such as nanocombs, nanorings, nanobelts, nanohelix, nanowires and nanocages as shown in Figure 2.2 (Yi *et al.*, 2005).

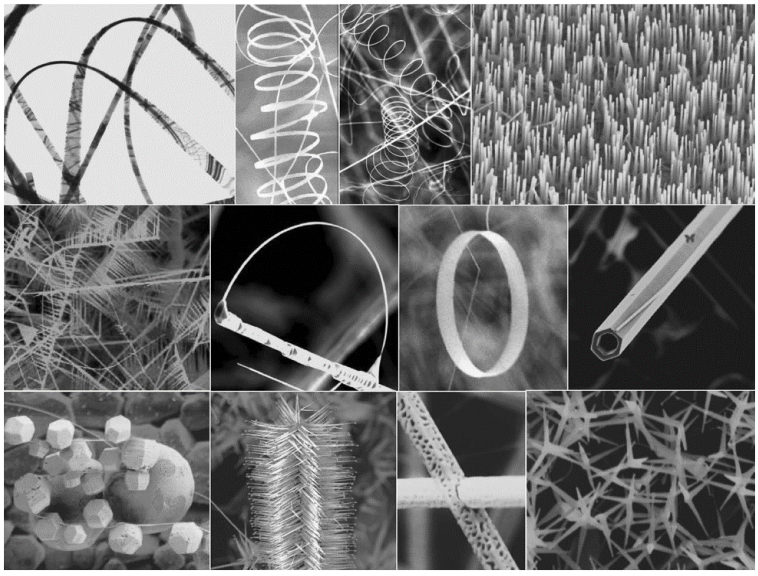

Figure 2.2: A collection of ZnO nanostructure synthesized under controlled conditions by thermal evaporation of solid powders (Yi *et al.*, 2005)

2.2.1 ZnO structure

ZnO is a II-VI compound semiconductor that generally exists in cubic rocksalt (B1), cubic zinc blende (B3) or hexagonal wurtzite (B4) structure with each of anion is bounded to four cations at the corners of tetrahedron, and vice versa as shown in Figure 2.3 (a), (b) and (c), respectively. Typically, tetrahedral coordination distinctive of sp^3 covalent bonding, but it also could have a substantial ionic character which tends to increase the band gap beyond that. Hence, ZnO ionicity resides at the borderline between the covalent and ionic semiconductors. Under an ambient condition, thermodynamically stable phase ZnO behaves in wurtzite structure, whereas zinc blende ZnO structure can be stabilized only by growing on a cubic

substrate (Morkoç and Özgür, 2009b). The wurtzite structure of ZnO composes of a hexagonal unit cell with two lattice parameters of a = 0.3296 nm which represents the basal plane, and c = 0.52065 nm which represents basal direction as shown in Figure 2.3 (d). In addition, the wurtzite ZnO belongs to space group of C^4_{6v} in the Schoenflies notation and $P6_3mc$ in the Hermann-Mauguin notation (Morkoç and Özgür, 2009b, Wang *et al.*, 2007b). Zinc oxide (ZnO) structure contains number of alternating planes composes of tetrahedrally coordinated $O^{2-}$and Zn^{2+} ions that are stacked alternately along c-axis with some surfaces can be terminated (Wang *et al.*, 2007a, Wang *et al.*, 2007b). Tetrahedral coordination of ZnO leads to a non-central symmetric structure.

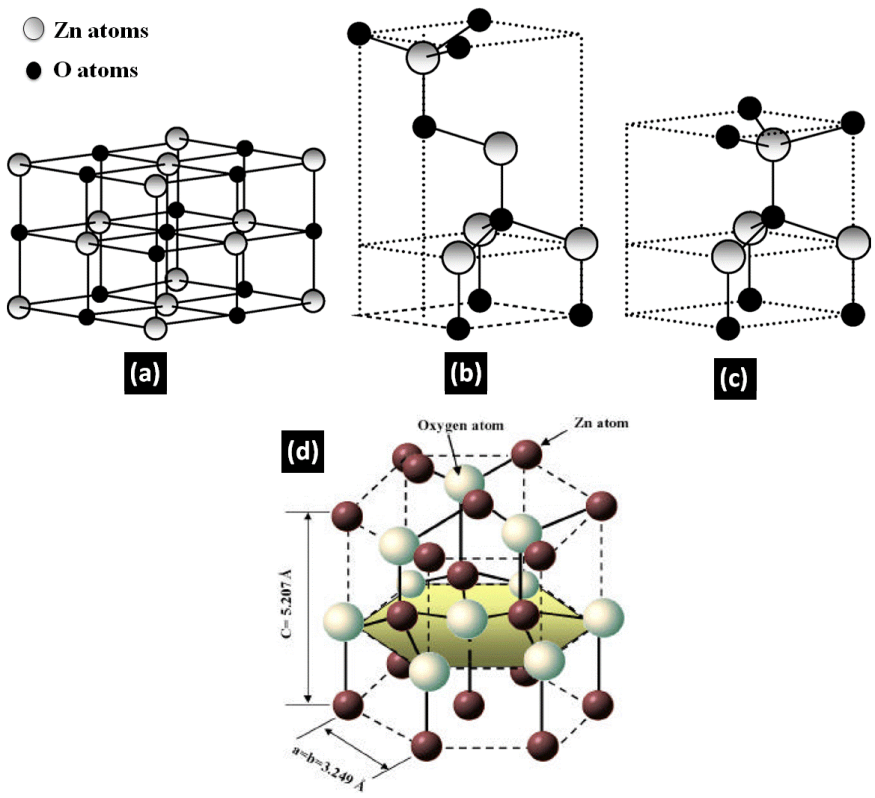

Figure 2.3: Stick-and-ball representation of ZnO crystal structure: (a) cubic rocksalt (B1), (b) cubic zinc blende (B3), and (c) hexagonal wurtzite (B4) (Morkoç and Özgür, 2009b) and (d) hexagonal wurtzite structure model of ZnO (Hahn, 2011)

2.2.2 Optical and electrical properties

ZnO is well known for its wide and gap of 3.37 eV with a large exciton binding energy of 60 meV at room temperature which ensures efficient excitonic emission in the UV range at room temperature (Liangyuan *et al.*, 2010, Wang *et al.*, 2004). High exciton energy compared to thermal energy at room temperature (k_BT~25 meV, where k_B is the Boltzmann's constant) ensures an efficient of UV emission at room temperature (Pauporté, 2009). Several reports have demonstrated the characteristic of photoluminescence (PL) spectra of ZnO with a typical of PL spectra of ZnO as shown in Figure 2.4 (a). Typically, PL spectra for ZnO compose of two parts which are ultraviolet (UV) emission peak at 380 nm that is attributed to the recombination of free excitons via band to band recombination and the second part is defect related band in visible range (VIS). The presence of defects that causes the formation of VIS emission peak could come from oxygen vacancies (V_O), zinc vacancies (V_{Zn}), oxygen interstitial (O_i), oxygen antisite (O_{Zn}) and other extrinsic impurities (Kondela *et al.*, 2010, Tan *et al.*, 2010). This property makes ZnO becomes a promising material to be used as UV photosensor. Wide band gap, high mobility, high breakdown voltage, high breakdown field strength and low noise generation makes ZnO suitable for a high power and temperature electronic devices. However, the electrical properties of ZnO is quite difficult to be determined due to large variance of samples quality that is available for example n-type doping has ~10^{20} electrons cm^{3-} while p-type doping has ~10^{19} holes cm^{3-}(Coleman and Jagadish, 2006).

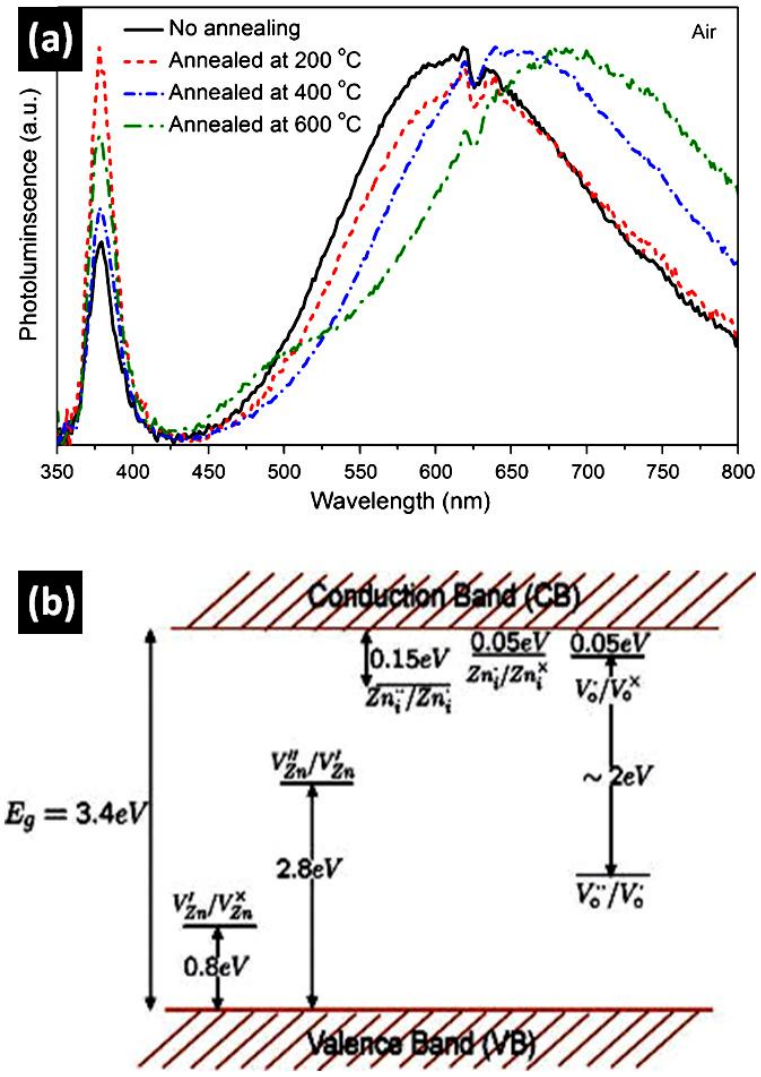

Figure 2.4: (a) Typical PL spectra of ZnO nanorods (Leung *et al.*, 2008) and (b) Energy levels of native defect in ZnO (Weintraub, 2010)

2.2.3 Thermal properties

In solid form, atoms in semiconductor at non-zero temperature vibrate at their equilibrium state and in a constant motion. However, the amplitude of vibration increases as a function of temperature. Hence, thermal properties of semiconductor including thermal coefficients, thermal conductivity and specific heat are dependent on temperature (Morkoç and Özgür, 2009b). Coleman and Jagadish (2006) reported that ZnO has thermal expansion coefficients of $\alpha_a = 4.31 \times 10^{-6} K^{-1}$ and $\alpha_c = 2.49 \times 10^{-6}$

K^{-1} at 300K, thermal conductivity of κ= 0.6-1 $Wcm^{-1}K^{-1}$ and specific heat, Cp=40.3 J mol^{-1} K^{-1} at a constant pressure.

Table 2.1: Properties of ZnO (Hahn, 2011, Min, 2003)

Lattice parameter at 300K a_0 c_0 c_0/a_0	 0.32495 nm 0.52069 nm 1.602
Density	5.67 g/cm^3 or $4.21x10^{19}$ ZnO molecules/mm^3
Melting point	1975 °C under pressure
Heat of fussion	4470 cal/mole
Thermal conductivity	0.6, 1-1.2 $W/cm^1°C^1$
Linear expansion coefficient	a_0: $6.5x10^{-6}$ cm^3/°C c_0 : $3.0x10^{-6}$ cm^3/°C
Static dielectric constant	8.656
Refractive index	2.008
Band gap	3.370 eV at room temperature 3.437 eV at -269.15 °C
Exciton binding energy	60 meV
Electron effective mass, m_e^* hall mobility at 300K	 0.24 200 cm^2/Vs
Hole effective mass, m_h^* hall mobility at 300K	 0.59 5-50 cm^2/Vs
Lattice energy	964 kcal/mole
Dielectric constant	ε_0 = 8.75, ε_∞ = 3.75
Piezoelectric coefficient	D_{33} = 12pC/N

2.3 Fabrication of ZnO nanorods

The formation of 1D ZnO nanostructure has attracted numerous attentions either for fundamental research or for potential device applications owing to its unique properties and quantum size effect. In addition, more efficient carrier transport will be gained compared to other nanostructures due to less grain boundaries, surface defects and disorder, and interface discontinuous (Chen *et al.*,

2009b). Hence, numerous methods have been carried out on synthesizing 1D ZnO nanostructure. Growth of ZnO nanostructures can be divided into physical approach whereby the growth process involves a high temperature environment (up to and close to 1000 °C) and chemical approach at low temperature (<100 °C) (Wang *et al.*, 2009, Willander *et al.*, 2009).

2.3.1 Molecular Beam Epitaxy

Generally the morphology of ZnO nanostructures is dependent on the growth condition and surface energy in which the geometric, electronic and defect of the surface of ZnO nanostructures will be influenced. This characteristic plays an important role for their potential application. Thus, to obtain high quality of grown ZnO, molecular beam epitaxy (MBE) technique has been widely used. MBE technique essentially consists of thermal energy molecular or atomic beam, which are produced by heating up the substrate at elevated temperature as shown in Figure 2.5 (a). Then, atoms migrate in an ultra high vacuum environment and impinge on the hot substrate surface. Through MBE technique better control and quality of grown ZnO will be obtained (Asghar *et al.*, 2010). Iwata *et al.*(2005) have used a-plane sapphire substrate to grow ZnO, which higher carrier mobility was obtained compared to grown on c-plane sapphire substrate. This is due to the reduction of electron by extended defects present (Iwata *et al.*, 2005). They also have demonstrate that ZnO structure growth on the sapphire substrate by MBE was influenced by ZnO polarity which O-polarity is dominant than Zn due to the difference in surface migration energy. Hence, 3D structure of ZnO was easily grown on sapphire substrate compared to other dimensional structure. However, to obtain a good performance in application, 1D structure of ZnO is preferable compared to 3D

structure. Lee *et al.* (2008) have proposed the use of periodically polarity inverted (PPI) ZnO templates to grow well ordered 1D ZnO on a sapphire substrate (Figure 2.5 (b)). By controlling the thickness of MgO buffer, O-polarity of ZnO film was formed on MgO thickness below 2.7 nm, whereas more than 2.7 nm Zn-polarity of ZnO film was obtained. In order to grow well aligned ZnO nanorods, Zn-polarity surface is preferable. Moreover, high density and dimension of nanorods also can be controlled by the polarity of template used. Even though well aligned and good crystal quality of ZnO nanorods was obtained on the sapphire substrate, but the use of sapphire substrate limit the use of ZnO nanorods for the electronic applications. Moreover, sapphire is not conductive and relatively expensive (Jian-Feng *et al.*, 2005).

Hong *et al.* (2009) used various types of substrate to grow ZnO nanorods via MBE technique including platinum layer/Si substrate, glass substrate, Si (100) substrate, Al_2O_3 (0001) substrate and GaN (0001) without catalyst-assisted growth. All ZnO samples exhibited a vertically aligned of nanorod arrays perpendicular on the substrates. They proposed the growth direction of ZnO nanorods is due to the highly anistropic surface energy of ZnO itself and not dependent on the substrate used. However, the density and surface morphology of ZnO is dependent on the crystal orientation of epitaxial film used. The use of GaN with crystal orientation of film of $(10\bar{1}2)$ will form a micropyramid arrays while GaN (0001) formed a nanorods structure. This shows that crystal orientation of substrate used have a strong epitaxial constraint on the growth mode of ZnO nanostructures (Hong *et al.*, 2009). MBE technique has provided a good quality of ZnO nanorods despite the use of different substrates. Single crystal of grown ZnO were observed by Asghar*et al*.

(2010), Hong *et al*. (2009), Iwata *et al*. (2005) and Jian-Feng*et al*. (2005). This observation shows an advantage of using MBE to grow ZnO nanorods since it provides a fine hetero-junction control with a clean environment that free form oxide layer formed. However, the use of MBE is limited as it is lower yield, hence not applicable for mass production (Xu and Wang, 2011).

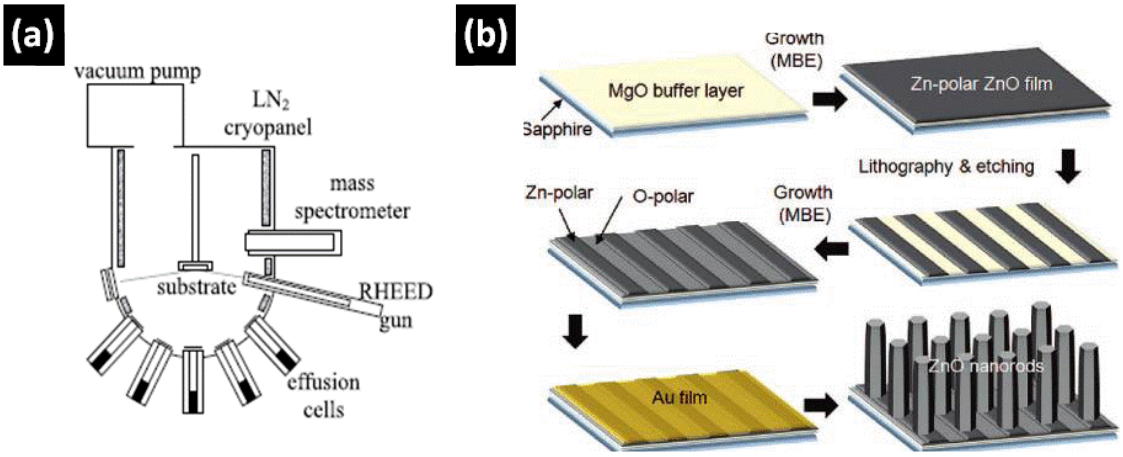

Figure 2.5: (a) A typical molecular beam epitaxy system (Rinaldi, 2002) and (b) schematic diagram of periodic polar inverted of ZnO templates for ordered ZnO nanorod arrays (Lee *et al.*, 2008)

2.3.2 Thermal evaporation/ Chemical Vapor Deposition

Generally, thermal evaporation and chemical vapour deposition (CVD) process involves the use of condensed or powder source materials that will be chemical decomposition and vaporized at high temperature to form Zn and ZnO_x vapors. The high quality and vertical aligned grown ZnO nanorods could be controlled by monitoring conditions such as temperature, pressure, atmosphere and substrate (Wang, 2004). The use of evaporation/CVD is believed to be a simple method to grow uniform and aligned small diameter ZnO nanostructures since the process is usually carried out in horizontal furnaces with tubular reaction chamber

constructed by an alumina tube or a quartz tube, rotary pump system, gas supply and control system. Khanlary *et al.* (2012) have demonstrated the effect of thermal evaporation temperature on the growth and morphology of ZnO. ZnO nanorods were grown on glass substrates by evaporation of Zn metallic at various temperatures from 450 to 650 °C. The dimension and density of nanorods increase linearly with increasing temperature up to 600°C. Further increase the temperature to 650 °C, ZnO dimension and density decreased due to the deformation of glass substrate used. Similar observation was obtained by Park *et al.* (2008) that show the effect of temperature (400 and 500 °C) on the growth of ZnO. They observed high evaporation temperature produced higher density of nanotips due to characteristic of Zn adatoms that has higher surface mobility and shorter surface life time resulting in preferred migration and desorption of the adsorbed Zn atoms from the surface area. However, ZnO grown at 500 °C has low intensity of (002) peak that showed a poor crystallinity.

Shalish *et al.* (2004) have demonstrated the dependence of dimension and density of ZnO nanowires on the PL spectra temperature as a function of evaporation temperature. They demonstrated that at high dimension of nanorods, high intensity of UV emission with a low deep-level emission while small diameter resulted in an increase of deep level intensity. The formation of high deep-level emission peak is due to the presence of singly ionized oxygen vacancy resulting from the recombination of electrons at the conduction band (Park *et al.*, 2008). Figure 2.6 show PL spectra obtained at different sizes of ZnO nanowires (Shalish *et al.*, 2004). The morphology of grown ZnO was also found to be dependent on the position of the substrates relative to the source including substrate upstream (Yang et al., 2002),

substrate downstream (Calestani *et al.*, 2011, Park *et al.*, 2008) and vertical/horizontal aligned substrate (Girtan *et al.*, 2008, Srivatsa *et al.*, 2011). The most widely used position is downstream whereby precursor source is placed before substrate. An accumulation of Zn and ZnO_x vapor before substrate was believed to have supersaturation before it reached and deposited onto substrates that promoted a high growth rate of ZnO (Calestani*et al*., 2011). Wang *et al.* (2012) have demonstrate the used of downstream position with difference distance position between substrate and source of 3 cm and 5 cm. The sample grown near the source consisted of axial nanorods with dimension of 1μm length and 50nm diameter, whereas the sample grown at 5 cm distance showed smaller dimension of nanorods. At relatively close distant (3 cm) concentration of Zn and ZnO_x vapor is high which enhanced the growth rate and dimension of ZnO as observed in sample of 3 cm. Umar *et al.* (2009) reported the growth of highly c-axis oriented ZnO nanorods was dependent on the heterogeneous nucleation. Two type of substrate were used; bare glass and glass with a ZnO coated film. They demonstrated that with the presence of ZnO film, ZnO nanorods grown perpendicular with substrate whereas when bare glass used multipod-like structures of ZnO were formed. There are also many derivatives of CVD terminology such as metal-organic chemical vapour depositions (MOCVD), organo metallic vapor phase epitaxy (OMVPE), laser chemical vapor deposition (LCVD) and plasma enhanced chemical vapor deposition (PECVD) (Creighton and Ho, 2001).

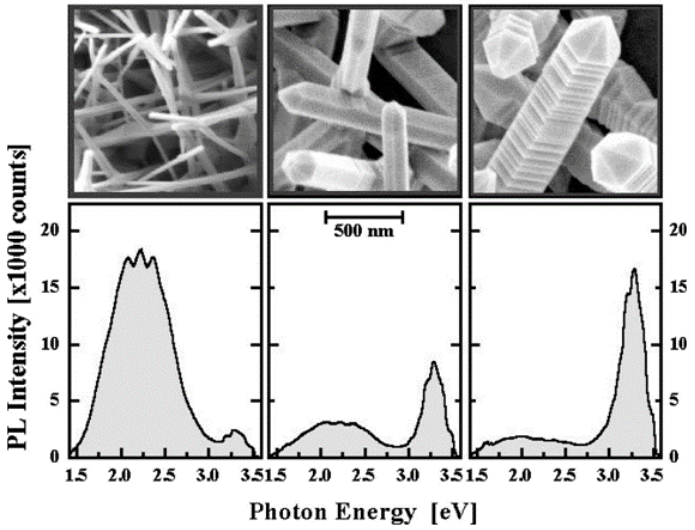

Figure 2.6: Photoluminescence spectra obtained from ZnO wires of three different sizes. SEM of the typical crystalline structures at each of the spots are shown above each of the spectra (Shalish *et al*., 2004)

2.3.3 Pulsed Laser Deposition

Pulsed laser deposition (PLD) technique uses a pulsed laser to ablate a target to produce the depositing flux. PLD has several distinct advantages such as instantaneous deposition rate, flexibility (multi-component target available), fast response, congruent evaporation, easy control thickness and simple system set up (Aziz, 2008, Hans-Ulrich Krebs *et al.,* 2003).The formation of nanostructure using PLD involves an ultrahigh vacuum (UHV) chamber and a high power excimer laser that is focused on the source target with a source target is placed at an angle of 45°. Atoms and ions ablated from the source target are deposited on substrate. The use of oxygen is crucial in order to grow ZnO nanostructures. Figure 2.7 (a) shows a schematic diagram of a typical laser deposition set-up (Hans-Ulrich Krebs *et al*., 2003). Several reports have demonstrated the influence of O_2 gas pressure commonly known as background pressure presence during PLD process (Liu *et al.*, 2006, Okada *et al.*, 2004, Okada *et al.*, 2005, Sakano *et al.*, 2008). In Okada et *al*. (2005), ZnO

nanorods were grown on a sapphire (0001) substrate at 700 °C at different O_2 gas pressure in the range from 0.1 to 20 Torr. They demonstrated that dimension of grown ZnO nanorods increased linearly with the increasing O_2 gas pressure. At high gas pressure, all nanorods fused together and the surface became flattened. Similar finding was observed in Liu *et al*. (2006). They demonstrated that at low gas pressure (5 Torr) a smaller diameter of nanorods formed. Further increased the background gas pressure to 20 Torr, nanorods started to coalescence and formed a continuous film.

Liu *et al*. (2006) studied the effect of substrate temperature in the range of 550 to 700 °C on morphology of ZnO nanorods. Diameter of ZnO nanorods became larger with increasing substrate temperature. They also demonstrated a linear relation between the substrate temperature, nanorods diameter and intensity of deep level band. For nanorods with larger diameter, depletion layer is important as the oxygen vacancies in nanorods lead to a stronger green emission (high intensity of deep level). Hence, higher deep level was observed in larger diameter nanorods (Liu *et al*., 2006). In Fuge *et al*. (2009) the effect of substrate temperature of seed layer was studied at 25 °C, 300 °C and 600 °C. ZnO nanorods were also grown at a constant substrate temperature of 600°C. The result shows a better alignment of ZnO grows with the increase of substrate temperature in seed layer which is due to the improvement of crystal quality seed layer properties as sufficient energy obtained which enable restructure in crystal lattice (Fuge *et al*., 2009). Sun *et al.* (2006) studied the effect of seed layer in ZnO growth in which the preparation of seed was done by PLD method at substrate temperature of 300 °C. They demonstrated the use of pre-deposited ZnO seed layer as a way to provide a nucleation sites for the

subsequent growth of ZnO. With the presence of ZnO seeds layer, higher density with longer and thinner nanorods was obtained.

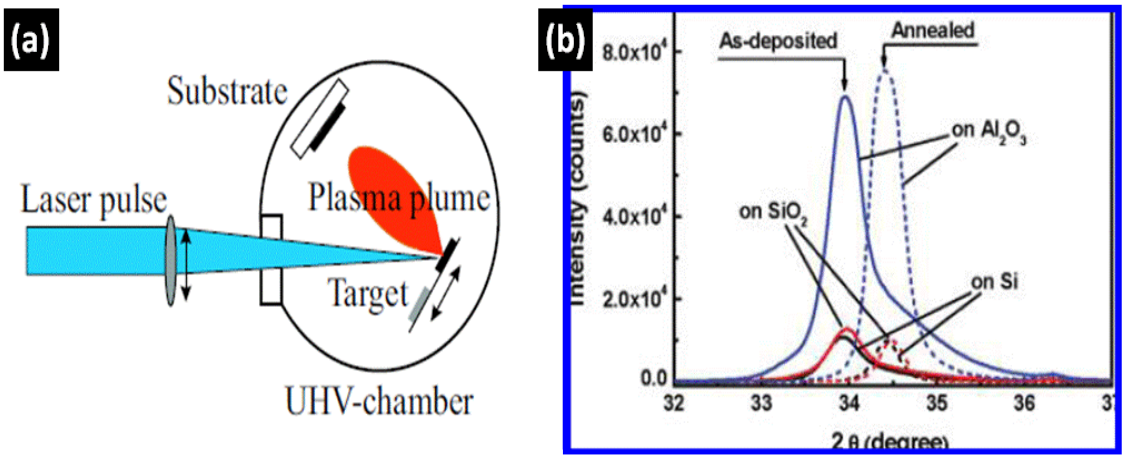

Figure 2.7: (a) Schematic diagram of a typical laser deposition set-up (Hans-Ulrich Krebs *et al.*, 2003) and (b) XRD patterns of the as-deposited and annealed ZnO films deposited on difference substrates showing the (002) diffraction peaks before and after annealing (Gao *et al.*, 2009)

2.3.4 Hydrothermal

Hydrothermal method can be defined as the process that utilizes single or heterogeneous phase reaction in aqueous or non-aqueous media where reaction happen above the room temperature and pressure more than 1 atm in a sealed container (Byrappa and Adschiri, 2007, Ngqondo, 2008). This condition results in the formation of vapor pressure from solution at a specific temperature and simultaneously forms autogeneous (self-developing) pressure within the reaction container. Beside the effect of temperature, the built up pressure inside reaction container is also influenced by percentage fill of the container and any dissolved salts (Yu and Qian, 2006). Shin *et al.* (2010) and Wu *et al.* (2010) have used an autoclave as a reaction container in order to provide continuous pressure. The use of Teflon